An Accurate Phase Measuring Deflectometry Method for 3D Reconstruction of Mirror-Like Specular Surface

Hao Han, Shiqian Wu
Key Laboratory of Metallurgical Equipment and Control Technology, Ministry of Education
Hubei Collaborative Innovation Center for Advanced Steels. Wuhan University and Science and Technology
Wuhan, China
e-mail: hh276125822@gmail.com, shiqian.wu@wust.edu.cn

Zhan Song*, Juan Zhao
Shenzhen Key Laboratory of Virtual Reality and Human Interaction Technology
Shenzhen Institutes of Advanced Technology, Chinese Academy of Sciences
Shenzhen, China
e-mail: {zhan.song;juan.zhao}@siat.ac.cn

***Abstract*—Measurement of specular surface shape is still a challenging task for existing 3D scanning techniques. In this paper, an accurate phase measuring deflectometry method is investigated for 3D reconstruction of mirror surfaces. To calibrate the system parameters, a standard flat mirror is used. By the reflected checkerboard pattern displayed by the LCD screen, the camera intrinsic parameters are calibrated firstly. The last orientation of calibration mirror is aligned as the reference plane. With such a calibration manner, intrinsic camera parameters, lens distortion and the LCD position can be determined efficiently. By displaying both horizontal and vertical Gray code plus sinusoidal shifting patterns on the LCD screen, dense surface gradient field is calculated with the proposed slope calculation method, and then integrated to retrieve precise 3D surface shapes. The experiments conducted with both flat and concave mirror surface demonstrate that high precision measurement results can be obtained.**

Keywords-phase measuring deflectometry; geometry calibration; slope calculation; 3D reconstruction

I. INTRODUCTION

Optical 3D shape metrology has been widely used in industrial inspection, reverse engineering, medical diagnosis and robot vision etc., due to its high speed, high accuracy and non-contact advantages. Off-the-shelf commercial 3D scanners like structured light system [1-3] and laser 3D scanners [4] can perform well in 3D measurement of diffuse surface or Lambertian surface. However, these scanning techniques are usually failed to obtain satisfied results for mirror-like specular surfaces due to strong reflectance. A usual solution is to coat the reflective surface with white powders before the application of 3D scanning. But such an operation will affect the measurement accuracy, and thus not suitable for high precision applications. Thus, the phase measuring deflectometry (PMD) technique has been developed [5-7].

Similar to the phase measurement profilometry (PMP) technique, 3D information of a mirror-like surface is modulated into the phase of a sinusoidal pattern. In the PMP method, the phase value only varies according to the surface height. But for the PMD method, the phase changes with both height and local slope of the surface, and the effect of the gradient is much larger. Major steps to implement a typical PMD system include optical system calibration [8-9], slope calculation [10-11] and slope integration [12-13]. The PMD techniques have been an important instrumentation for the applications such as measurements of intraocular lens [14], big mirrors for astronomical telescopes [15], aspheric surfaces [16] and even free-form surfaces [5] at different stages of optical fabrication.

In this paper, an accurate PMD method is investigated for the 3D measurement of mirror-like surfaces. In the calibration, we calibrate the camera using a checkerboard pattern shown by an LCD display. By changing the flat mirror to different orientations, several images are captured for calibration. The last orientation is aligned as the reference plane. Thus, the intrinsic camera parameters and the LCD position can be determined simultaneously. Then horizontal and vertical gray code plus sinusoidal patterns are displayed and captured to calculate the slope along X-axis and Y-axis of the world coordinate. Finally, direction of the slope is analyzed and transferred for integration and 3D reconstruction. The paper is organized as follows. Section II presents the procedures of calibration and slope calculation in details. In Section III, experiment and evaluation are showed and discussed to verify the proposed method. Conclusion and future work are drawn in Section IV.

II. THE PROPOSED PMD METHODOLOGY

The proposed PMD metrology system is shown in Fig. 1, which contains a CCD camera, an LCD display, and the target mirror-like surface. The displayed sinusoidal patterns by LCD screen are observed by the CCD camera after the reflection of specular surface. Then the surface x-slope and y-slope are calculated by the system geometry model and calibration parameters. Finally, the slope is integrated to obtain the 3D shape of target surface.

978-1-7281-2662-3/19/$31.00 ©2019 IEEE
DOI 10.1109/ICoIAS.2019.00010

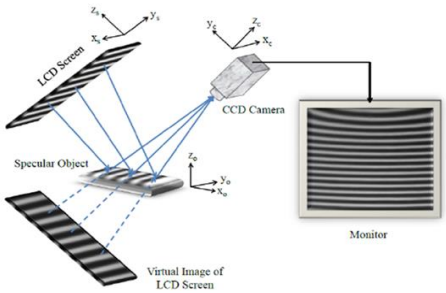

Figure 1. The proposed PMD metrology system contains a CCD camera, an LCD screen, and the target with mirror-like surface.

A. Calibration of the PMD System

The calibration process of a PMD system can be divided into the camera calibration and geometry calibration. Inspired by the LCD-based structured light calibration method in [17], the camera is focused on the object surface instead of the virtual image of LCD screen in the proposed PMD system. A checkerboard pattern with asymmetric dots is designed and displayed on the LCD screen. By changing posture of the standard flat mirror, different views of the patterns can be acquired for camera calibration [18]. The last position is regarded as the reference plane. By using this method, intrinsic camera parameters, lens distortions and LCD position can be determined more efficiently.

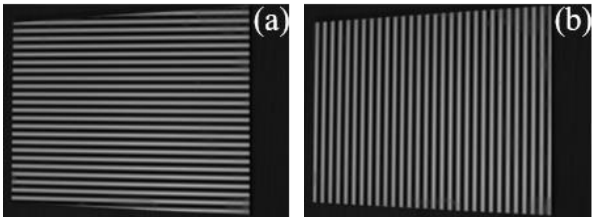

Figure 2. A series of (a) horizontal and (b) vertical sinusoidal patterns are displayed by the LCD screen and captured by the camera.

To calculate slope of each image point, correspondence between camera pixel, LCD pixel and surface point has to be determined. According to the PMP principle, a series of horizontal and vertical sinusoidal fringe patterns are created and displayed to illuminate the target surface and the captured images as shown by Fig. 2 can be represented as,

$$I_n(x,y) = a(x,y) + b(x,y)\cdot\cos[\varphi(x,y) + \frac{2n\pi}{N}], n = 0,1,...,N-1. \quad (1)$$

where $a(x,y)$, $b(x,y)$, $\varphi(x,y)$ indicates the background, modulation and phase of x or y directional fringes respectively. N is the step of phase shifting [19]. The wrapped phase $\varphi(x,y)$ can be calculated as,

$$\varphi(x,y) = \arctan\frac{\sum_0^{N-1} I_n \sin\left(\frac{2n\pi}{N}\right)}{\sum_0^{N-1} I_n \cos\left(\frac{2n\pi}{N}\right)} \quad (2)$$

After the fringe demodulation, the phase values are wrapped within [- π, π] because of the range value of inverse tangent function. In order to calculate slopes from the phase values, the global Gray code patterns are used for phase unwrapping. Specifically, both positive and negative gray code patterns are used to enhance the robustness and accuracy of the decoding procedure.

The absolute phase $\phi(x,y)$ can be calculated as,

$$\phi(x,y) = \varphi + 2k\pi \quad (3)$$

where k indicates the order of the stripes. Once we worked out the absolute phase ϕ_x for vertical fringe patterns and ϕ_y for horizontal fringe patterns, then the corresponding LCD pixel can be determined since the period of the fringe pattern on the screen is a known parameter as follows

$$\begin{pmatrix} x_s \\ y_s \end{pmatrix} = \begin{pmatrix} \phi_x \\ \phi_y \end{pmatrix} \cdot \frac{T}{2\pi} \cdot unit \quad (4)$$

where (x_s, y_s) is the coordinates of LCD pixel, T is the pixel period of sinusoidal fringe, and *unit* refers to the LCD pixel size. By locating the centroid of checker points and interpolating from the measured phase ϕ_x and ϕ_y , the checker points' measured phase can be received as ϕ_x^m and ϕ_y^m , the nominal phase can easily be known as ϕ_x^n and ϕ_y^n , the calculated reprojection error is show by Fig. 3, where the absolute mean error is only 0.0277. Thus, phase value on the reference can be obtained and expressed as ϕ_x^r and ϕ_y^r .

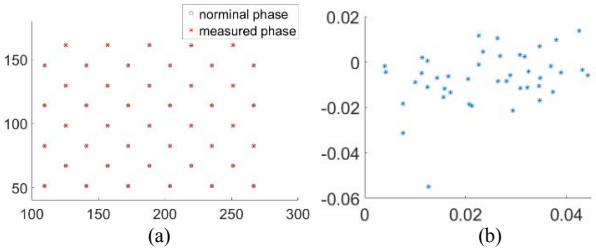

Figure 3. (a) Norminal and measured phase values on the calibration feature points; (b) Reprojection error of the phase values.

To find the correspondence between camera pixel and the flat mirror point, a checkerboard need be placed on the flat mirror to get the extrinsic parameters of the reference. By applying the SVD plane fitting algorithm, the reference plane equation can be expressed as:

$$A_r x + B_r y + C_r z + D_r = 0 \quad (5)$$

To obtain the 3D ray that passes through a position (u,v) on the image plane, we apply the following projective transformation using the camera parameters:

$$\begin{bmatrix} sRx \\ sRy \\ sRz \\ s \end{bmatrix} = [K_{\text{int}} \cdot K_{ext}]^{-1} \begin{bmatrix} u \\ v \\ 1 \end{bmatrix} \tag{6}$$

where the vector of the ray (Rx, Ry, Rz) is up to a scale factor s, K_{int} and K_{ext} are camera intrinsic and extrinsic parameters, then we have,

$$A_r(sRx) + B_r(sRy) + C_r(sRz) + D_r = 0 \tag{7}$$

By solving (7), we can establish the correspondence between camera pixel and the flat mirror point.

B. Slope Calculation and Surface Reconstruction

To calculate x and y slope of the specular surface, the same sequence of gray code and sinusoidal patterns are displayed by the LCD screen, then reflected by the target surface and captured by the camera. Defining the absolute phase values as ϕ_x^w and ϕ_y^w, the two-directional phase differences $\Delta\phi_x = \phi_x^w - \phi_x^r$ and $\Delta\phi_y = \phi_y^w - \phi_y^r$ are used to calculate x-slope and y-slope.

Fig. 4(a) shows the geometric model of the PMD system. Assuming the camera as a light source which obeys ray-tracing model, a light ray emitted by the pixel P hits the reference plane at S and then reflected to F_1 on the LCD screen. When measuring the objects, the same light emitted by pixel P hits object surface at W and reflected to F_2 in the end. F_{21x} and F_{21y} are the projected points of F_2 along X_L and Y_L in the LCD coordinates, that satisfies:

$$\begin{cases} \overrightarrow{F_1F_{21x}} = \Delta\phi_x \cdot \dfrac{T}{2\pi} \cdot unit \\ \overrightarrow{F_1F_{21y}} = \Delta\phi_y \cdot \dfrac{T}{2\pi} \cdot unit \end{cases} \tag{8}$$

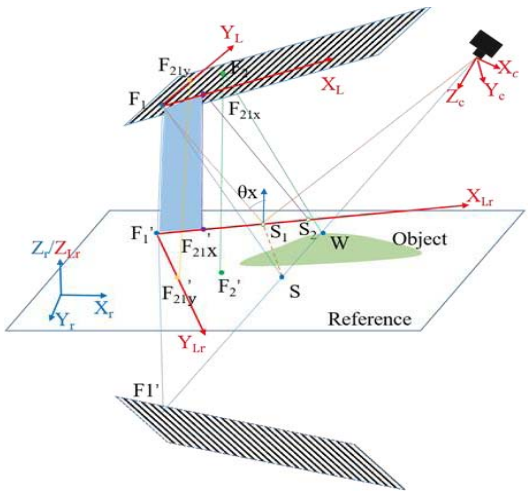

(a)

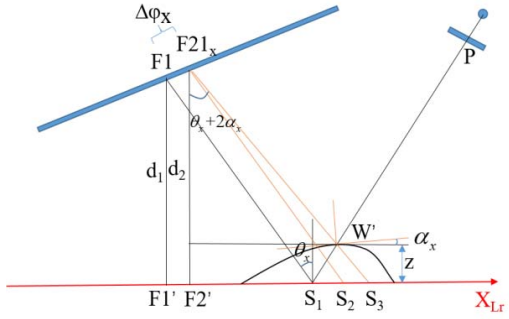

(b)

Figure 4. (a) 3D geometric model of the proposed PMD system; (b) 2D slop calculation under the LCD refrence frame.

In Fig. 4(a), $F_1', F_2', F_{21x}', F_{21y}'$ are the projected points of $F_1, F_2, F_{21x}, F_{21y}$ to the reference plane. Then we project the 3D model to the plane consisted by quadrangle $F_1F_1'F_{21x}'F_{21x}$ along Y_{Lr}-direction, S_1, W' are the projected points of S and W, as shown by Fig. 4(b). The x-slope g_x^{Lr} is calculated by (9) and (10).

$$\tan(\theta_x + 2\alpha_x) = \frac{d_2 \tan\theta_x + z\tan\theta_x - \overline{S_1S_2}}{d_2 - z} \tag{9}$$

$$g_x^{Lr} = \tan\alpha_x \tag{10}$$

The y-slope g_y^{Lr} can be calculated similarly. Note that an issue arises during the perspective projection. Due to the fact that the y-axis of LCD cannot be the same direction as y-axis of the reference plane in the actual experiment, so the perspective projection of X_L and Y_L to the reference plane, labeled as X_{Lr} and Y_{Lr}, are inconsistent with X_r and Y_r. In addition, X_{Lr} may not be perpendicular to Y_{Lr}. As described in [7], the gradient data of the object should theoretically be a conservative field. Actually, the system error and improper assumptions make it a non-conservative field. Hence, the g_x^{Lr} and g_y^{Lr} should be transformed to the gradient g_x^r and g_y^r of X_r-axis and Y_r-axis by the definition of the directional derivative as

$$\frac{\partial f}{\partial l} = \frac{\partial f}{\partial x}\cos\varphi + \frac{\partial f}{\partial y}\sin\varphi = \left\{\frac{\partial f}{\partial x}, \frac{\partial f}{\partial y}\right\} \cdot \{\cos\varphi, \sin\varphi\} \tag{11}$$

Equation (11) is further expressed as:

$$\begin{pmatrix} g_x^{Lr} \\ g_y^{Lr} \end{pmatrix} = \begin{pmatrix} \cos\varphi_{X_{Lr}} & \sin\varphi_{X_{Lr}} \\ \cos\varphi_{Y_{Lr}} & \sin\varphi_{Y_{Lr}} \end{pmatrix} \cdot \begin{pmatrix} g_x^r \\ g_y^r \end{pmatrix} \tag{12}$$

By solving (12), more accurate g_x^r and g_y^r can be obtained. Once the two-directional gradient data are acquired, the slope integration method [20] is applied to reconstruct 3D model of the surface.

III. EXPERIMENT AND EVALUATION

The established PMD metrology system is shown in Fig.5. The camera resolution is 2080×1552 pixel and the pixel size is 2.5μm. The sinusoidal structured light patterns are displayed by one HP24es 23.8-inch LCD screen, which has a resolution of 1920×1080 and the pixel pitch is 0.2745mm. Distance between the target and screen is about 350 mm.

In our experiment, a flat mirror of ϕ100 mm and a concave mirror of ϕ40 mm are used. Focal length of the concave mirror is 100 mm. After calibration of the PMD system, the flat mirror is reconstructed firstly, and the results are shown in Fig. 6. By fitting the reconstructed plane via least square means, the peak-valley value is about 15 um, and the STD error is about 2.98 um.

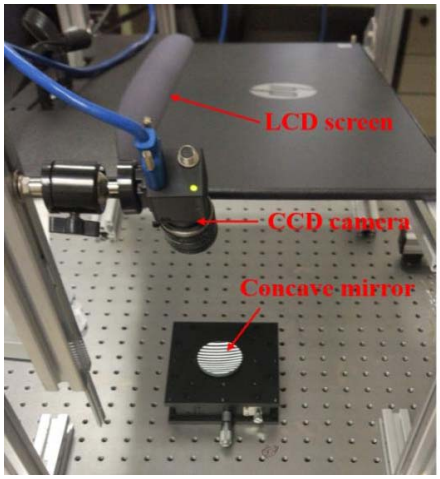

Figure 5. The experimental PMD system.

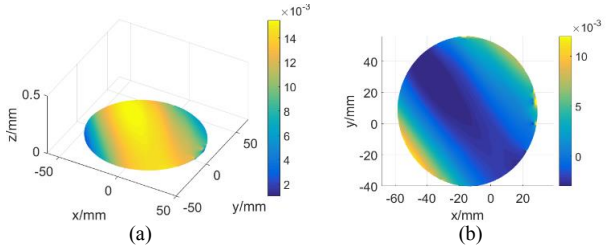

Figure 6. (a) flat mirror result (b) the plane fitting error

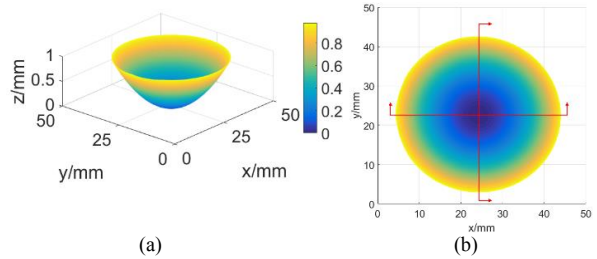

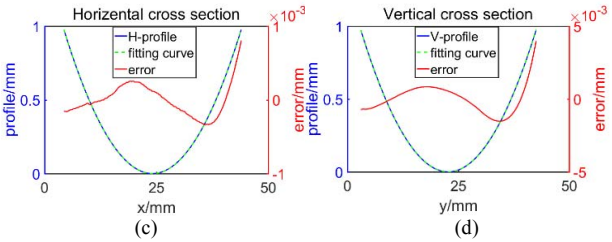

Figure 7. (a) Reconstructed 3D model of the concave mirror; (b) 3D mdoel under top view; (c) horizontal cross section and circle fitting result; (d) vertical cross section and cirlce fitting result;

Fig. 7 shows the reconstruction result of the concave mirror. 3D model of the mirror surface is shown in Fig. 7(a). From the data provided by the manufacturer, radius of mirror curvature is 200 mm, with a tolerance of ±2%. To evaluate the reconstruction precision, we extract the horizontal and vertical cross section through the valley point as shown in Fig. 7(b). Then we use circle fitting algorithm to fit the profile and acquire the fitting radius $R_H = 201.55$ mm and $R_V = 201.10$ mm, shown in Fig. 7(c) and Fig. 7(d). The blue solid line is the original profile, green dash line is the fitting curve, and the fitting error is depicted by the red line. We see that, both section lines are well overlapped with the fitting curves. The STD error is 0.22um in horizontal and 0.96 um in vertical. With above experiments, precision of the proposed PMD measurement system can be fully demonstrated.

IV. CONCLUSION AND FUTURE WORK

This paper presents an accurate PMD-based method for 3D reconstruction of mirror-like specular surface. A standard flat mirror is used for the system calibration. By changing the flat mirror to several different orientations, the camera can be precisely calibrated. The last orientation of flat mirror is aligned as the reference plane. With such a calibration manner, intrinsic camera parameters, lens distortion and the LCD position can be determined efficiently. In the 3D scanning stage, both horizontal and vertical sinusoidal patterns are displayed by the LCD and captured to calculate the slope along X-axis and Y-axis of the world coordinate. By calculating surface slopes and using gradient integration method, 3D model of the specular surface can be reconstructed. In the 3D reconstruction experiments, the flat mirror is used firstly, where a standard deviation of only 2.9 um was obtained. Future work can address how to deal with the mirror-like surfaces with large curvatures and how to improve the measurement accuracy furtherly.

ACKNOWLEDGMENT

This work was supported in part by the National Key R&D Program of China (No. 2017YFB1103602), Shenzhen Key Laboratory (No. ZDSYS201605101739178), and the National Natural Science Foundation of China (Nos. 61775172, 61773363, 51705513).

REFERENCES

[1] Z. Song, R. Chung, X. Zhang, "An Accurate and Robust Strip-edge based Structured Light Means for Shiny Surface Micro-measurement in 3D," IEEE Trans on Industrial Electronics, vol.60, Mar.2012, pp.1023-1032, doi:10.1109/TIE.2012.2188875.

[2] Z. Song. "Recent Progresses on Real-Time 3D Shape Measurement Using Digital Fringe Projection Techniques," Optics & Lasers in Engineering. vol.48, Feb. 2010, pp.149-158, doi:10.1016/j. patcog.2009.03.008.

[3] J. Salvi, S. Fernandez, T. Pribanic, X. Llado, "A State of the Art in Structured Light Patterns for Surface Profilometry," Optics & Lasers in Engineering, vol. 43, Aug. 2010, pp. 2666-2680, doi:10.1016/j.patcog.2010.03.004.

[4] Q. Wu and D. Xu and W. Zou, "A Survey on Three-Dimensional Modeling Based on Line Structured Light Scanner," Proceedings of the 33rd Chinese Control Conference, Jul.2014, pp.7439d-7444, doi:10.1109/ChiCC.2014.6896237.

[5] M. Knauer, J. Kaminski, G. Hausler, "Phase Measuring Deflectometry: A New Approach to Measure Specular Free-Form Surfaces," Proc. SPIE 5457, Optical Metrology in Production Engineering, Sep 2004, doi:10.1117/12.545704.

[6] L Huang, M Idir, C Zuo, "Review of Phase Measuring Deflectometry," Optics & Lasers in Engineering, vol.107, Aug.2018, pp.247-257, doi:10.1016/j.optlaseng.2018.03.026

[7] T. Bothe, W. Li, C. von Kopylow, and W. Juptner, "High Resolution 3D Shape Measurement on Specular Surfaces by Fringe Reflection," Proceedings of SPIE-the International Society for Optical Engineering, vol.5457, Sep.2004, pp.411-422, doi:10.1117/12.545987.

[8] E Kewei, D Li, L Yang, "Novel Method for High Accuracy Figure Measurement of Optical Flat," Optics & Lasers in Engineering, vol.88, Jan.2017, pp.162-166, doi:10.1016/j.optla- seng.2016.07.011.

[9] H Ren, F Gao, X Jiang, "Iterative Optimization Calibration Method for Stereo Deflectometry," Optics Express, vol.23, Sep.2015, pp. 22060-22068, doi:10.1364/OE.23.022060

[10] H. Zhang, S. Han, S. Liu, S. Li, L. Ji, and X. Zhang, "3D Shape Reconstruction of Large Specular Surface," Applied Optics, vol.51, Oct.2012, pp.7616-7625, doi:10.1364/AO.51.007616.

[11] C. Guo, X. Lin, A. Hu, and J. Zou, "Improved Phase-Measuring Deflectometry for Aspheric Surfaces Test," Applied Optics, vol.55, Mar. 2016, pp.2059-2064, doi:10.1364/AO.55.002059.

[12] L. Huang, M. Idir, C. Zuo, K. Kaznatcheev, L. Zhou, A Asundi, "Comparison of Two-Dimensional Integration Methods for Shape Reconstruction from Gradient Data," Optics & Lasers in Engineering, vol.64, Jul.2015, pp 1-11, doi:10.1016/j.optlaseng.2014.07.002.

[13] M. Li, D. Li, Ch. Jin, K. E, X. Yuan, Z. Xiong, and Q. Wang, "Improved Zonal Integration Method for High Accurate Surface Reconstruction in Quantitative Deflectometry," Applied Optics, vol. 56, Mar.2017, pp. F144-F151, doi:10.1364/AO.56.00F144.

[14] A. Speck, B. Zelzer, M. Kannengießer, A. Langenbucher, and T. Eppig, "Inspection of Freeform Intraocular Lens Topography by Phase Measuring Deflectometric Methods," Applied Optics, vol.52, Jun.2013, pp. 4279-4286, doi:10.1364/AO.52.004279.

[15] P. Su, R. E. Parks, L. Wang, R. P. Angel, and J. H. Burge, "Software Configurable Optical Test System: A Computerized Reverse Hartmann Test," Applied Optics, vol.49, Aug.2010, pp.4404-4412, doi:10.1364/AO.49.004404.

[16] Y. Xiao, X. Su, W. Chen, and Y. Liu, "Three-Dimensional Shape Measurement of Aspheric Mirrors with Fringe Reflection Photogrammetry," Applied Optics, Vol. 51, Jan.2012, pp.457–464, doi:10.1364/AO.51.000457.

[17] Z. Song and R. Chung. "Use of LCD Panel for Calibrating Structured-Light-Based Range Sensing System," IEEE Transactions on Instrumentation & Measurement, vol. 57, Nov. 2008, pp. 2623-2630, doi:10.1109/TIM.2008.925016.

[18] Z. Zhang, "A Flexible New Technique for Camera Calibration," IEEE Transactions on Pattern Analysis & Machine Intelligence, vol.22, Nov. 2000, pp.1330-1334, doi:10.1109/34.888718.

[19] C. Zuo, S. Feng, L. Huang, T. Tao, W. Yin and Q. Chen, "Phase Shifting Algorithms for Fringe Projection Profilometry: A Review," Optics & Lasers in Engineering, vol.109, May 2018, pp.23-59, doi:10.1016/j.optlaseng.2018.04.019

[20] L. Huang, J. Xue, B. Gao, C. Zuo, M. Idir, "Iterative Optimization Calibration Method for Stereo Deflectometry," Applied Optics, vol. 56, Jan.2017, pp. 22060-22068, doi:10.1364/AO.56.005139